

Outline

- 1 Introduction
- 2 Early Pattern Selection
- 3 Summary

Reaction-diffusion Systems

Reaction-diffusion describes the process in which multiple participating chemicals or agents react with each other, while simultaneously diffusing or spreading through a liquid or gaseous medium.

- Typically modeled with either local or nonlocal diffusion terms
- Includes nonlinear terms that incorporate the effects of the reaction kinetics

Pattern formation in Reaction-diffusion Systems

Patterns such as spots or stripes have been experimentally observed in:

- CIMA reaction in a gel reactor [1, 9],
- CDIMA reaction [2],
- BZ reaction dispersed in a water-in-oil microemulsion system [10].

The corresponding models have also been shown to produce both spots and stripes:

- CIMA reaction [4],
- CDIMA reaction [11],
- BZ reaction [5].

Local Reaction-diffusion Model

Subject to periodic boundary conditions, consider

$$\begin{aligned}u_t &= \epsilon \Delta u + f(u, v), \\v_t &= d\epsilon \Delta v + g(u, v),\end{aligned}\tag{1}$$

- $\Omega \subset \mathbb{R}^n$ for $n \in \{1, 2, 3\}$

Nonlocal Effects

- The local models do not account for any nonlocal diffusion effects.
- Using a nonlocal feedback illuminating source, Hildebrand, Skødt and Showalter [3] experimentally showed the existence of novel spatiotemporal patterns in the BZ reaction.
- Subject to periodic boundary conditions, we consider a reaction-diffusion system of the more general form

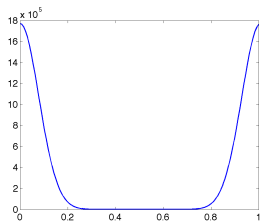
Mixed Reaction-diffusion Model

Subject to periodic boundary conditions, consider

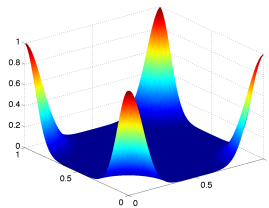
$$\begin{aligned}u_t &= \epsilon(\beta\Delta u + (1 - \beta)(J_c(u) - \hat{J}_0)) + f(u, v), \\v_t &= d\epsilon(\beta\Delta v + (1 - \beta)(J_c(v) - \hat{J}_0)) + g(u, v),\end{aligned}\quad (2)$$

- $\Omega \subset \mathbb{R}^n$ for $n \in \{1, 2, 3\}$
- $0 \leq \beta \leq 1$
- $J_c(u(x, t)) = J * u$
- $\hat{J}_0 = \int_{\Omega} J(x) dx$
- $\epsilon^\theta J$ is ϵ -independent for $\theta \in \mathbb{R}$.
- $\epsilon^\theta J : \mathbb{R}^n \rightarrow \mathbb{R}$ is smoothly periodic on Ω .

The Kernel J



(a) 1d Kernel



(b) 2d Kernel

Linearization

$$U' = \mathcal{H}_\epsilon U = \epsilon D \mathcal{J} U + B U, \quad (3)$$

where

$$D = \begin{pmatrix} 1 & 0 \\ 0 & d \end{pmatrix}, \quad (4)$$

$$\mathcal{J} = \beta \begin{pmatrix} \Delta & 0 \\ 0 & \Delta \end{pmatrix} + (1 - \beta) \begin{pmatrix} J_c & 0 \\ 0 & J_c \end{pmatrix}, \quad (5)$$

$$B = \begin{pmatrix} f_u(\bar{u}_0, \bar{v}_0) & f_v(\bar{u}_0, \bar{v}_0) \\ g_u(\bar{u}_0, \bar{v}_0) & g_v(\bar{u}_0, \bar{v}_0) \end{pmatrix}, \quad (6)$$

where $U = (u, v)^T$.

Focus of Work

The goal of this work is to analyze the mixed reaction-diffusion system.

- Early pattern selection for $\theta < 1$, $0 < \beta \leq 1$
- Early pattern selection for $\theta = 1$

Outline

- 1 Introduction
- 2 Early Pattern Selection
- 3 Summary

Turing Instability

In the absence of diffusion, the homogeneous equilibrium (\bar{u}_0, \bar{v}_0) is stable. Otherwise, the homogeneous equilibrium is unstable.

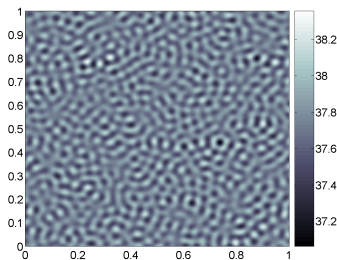


Figure: Pattern resulting from Turing instability, $\epsilon = 1 \times 10^{-5}$,
 $time = 4 \times 10^{-4}$, and $\beta = 1.0$

Almost Linear Behavior

- Let (u, v) and (u_{lin}, v_{lin}) be the solutions to the system and its linearized counterpart, respectively.
- For solutions that begin within an arbitrarily small ϵ -dependent distance r_ϵ to (\bar{u}_0, \bar{v}_0) and exit the neighborhood at a distance of $R_\epsilon > r_\epsilon$, the relative distance

$$\frac{\|(u(t), v(t)) - (\bar{u}_0, \bar{v}_0) - (u_{lin}, v_{lin})\|_{**}}{\|(u_{lin}(t), v_{lin}(t))\|_{**}},$$

is proportional to an ϵ -dependent threshold.

In particular, r_ϵ and the relative distance decrease to zero as $\epsilon \rightarrow 0$, whereas R_ϵ grows as $\epsilon \rightarrow 0$. This behavior is called **almost linear behavior** .

Stable/Unstable Spaces

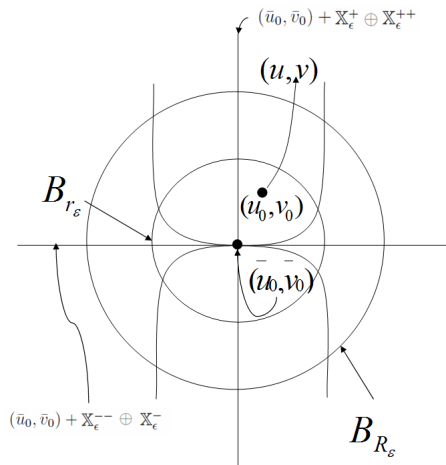


Figure: Schematic of Early pattern selection

Assumptions

- Let Ω be a closed rectangular subset of \mathbb{R}^n for $n \in \{1, 2, 3\}$.
- Let the kernel $J \in C^1(\bar{\Omega})$ be such that the following are true:
 - J is smoothly periodic on Ω .
 - $\epsilon^\theta J$ is ϵ -independent for $\theta \in \mathbb{R}$.
 - $\hat{J}_0 - \hat{J}_k \geq 0$ for all $k \geq 1$.
 - Suppose that the periodic extension of J is even.
- Assume that $f, g : \mathbb{R}^2 \rightarrow \mathbb{R}$ are $C^{1+\delta}$ -smooth functions
- Assume that $(\bar{u}_0, \bar{v}_0) \in \mathbb{R}^2$ is a homogeneous equilibrium of the system.
- Suppose that the homogeneous equilibrium of System 2 exhibits Turing instability and that the linearization yields real eigenvalues.

Early Pattern Results for $\theta < 1$, $0 < \beta \leq 1$ (New)

Theorem

Let $\epsilon < \epsilon_0$. Consider System 2, where $0 < \beta \leq 1$. Assume that the domain Ω is a rectangular domain of \mathbb{R}^n , where $n = \{1, 2, 3\}$. The kernel function $J \in C^1(\bar{\Omega})$, where J is smoothly periodic, $\epsilon^\theta J$ is ϵ -independent for $\theta \in \mathbb{R}$, $\hat{J}_0 - \hat{J}_k \geq 0$ for all $k \geq 1$ and the extension of J is even. Suppose that the nonlinearities f and g are sufficiently smooth and that the homogeneous equilibrium (\bar{u}_0, \bar{v}_0) is unstable for ϵ_0 . Finally, let (u, v) and (u_{lin}, v_{lin}) be the solutions to System 2 and its linear approximation at the homogeneous equilibrium, respectively.

The solution (u, v) possesses almost linear behavior.

Early Pattern Results for $\theta = 1$ (New)

Suppose that $\epsilon(1 - \beta)\hat{J}_0 > s_r$, where (s_l, s_r) defines the interval for which the eigenvalues of the linearization are unstable. Furthermore, suppose that there is at least one $\epsilon(1 - \beta)(\hat{J}_0 - \hat{J}_k) \in (s_l, s_r)$.

- The nonlinearity is no longer bounded above by an ϵ -dependent bound as in the $\theta < 1$ case.
- We provide numerics for $\beta = 0$ that suggest the almost linear results do not hold.

Early Pattern Results for $\theta = 1$ (New)

- For 20 simulations, the distance between the nonlinear solution and the homogeneous equilibrium was measured when the solutions deviated from each other.
- Deviation means the distance between the linear and nonlinear solutions relative to the norm of the linear solution reached a threshold of $.25\epsilon^{1/4}$.
- For each simulation, random initial conditions were selected to be within a distance $\epsilon^{1/2}$ of the homogeneous equilibrium.
- The distances were measured with respect to the $\|\cdot\|_{**}$.

Early Pattern Results for $\beta = 0$

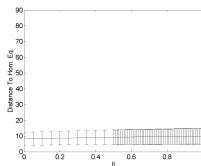
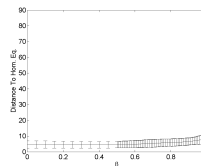
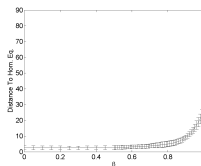
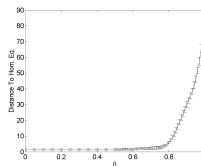
(a) $\epsilon = .01$ (b) $\epsilon = .001$ (c) $\epsilon = .0001$ (d) $\epsilon = .00001$

Figure: Demonstration of Increased Nonlinear Behavior for Nonlocal System

Techniques for Proving Early Pattern Selection

To prove this result, the abstract theory and techniques developed for the Cahn-Hilliard equation found in [6], [7] are used. The theory requires an abstract evolution equation of the form

$$U_t = \mathcal{H}_\epsilon U + F(U),$$

on some appropriate function space \mathbb{X} that satisfies the following assumptions.

Techniques for Proving Early Pattern Selection

- (H1) The operator $-\mathcal{H}_\epsilon$ is a sectorial operator on \mathbb{X} .
- (H2) There exists a decomposition $\mathbb{X} = \mathbb{X}^{--} \oplus \mathbb{X}^- \oplus \mathbb{X}^+ \oplus \mathbb{X}^{++}$, such that all of these subspaces are finite except \mathbb{X}^{--} , and such that the linear semigroup corresponding to $U_t = \mathcal{H}_\epsilon U$ satisfies several dichotomy estimates.
- (H3) The nonlinearity $F : \mathbb{X}^\alpha \rightarrow \mathbb{X}$ is continuously differentiable, and satisfies both $F(\bar{u}_0, \bar{v}_0) = 0$ and $DF(\bar{u}_0, \bar{v}_0) = 0$.

Techniques for Proving Early Pattern Selection

- For $0 < \beta \leq 1$, $\mathbb{X}^\alpha = \mathbb{H}_{per}^{2\alpha}(\Omega)$, where $\mathbb{H}_{per}^{2\alpha}(\Omega) = H_{per}^{2\alpha}(\Omega) \times H_{per}^{2\alpha}(\Omega)$ and $H_{per}^{2\alpha}(\Omega)$ is the standard Sobolev space of Ω -periodic functions.
- If (H1), (H2) and (H3) are true, then there exists an exponentially attracting invariant manifold that is tangent to $\mathbb{X}^- \oplus \mathbb{X}^+ \oplus \mathbb{X}^{++}$ [7, Lemma 2.1]. However, [7, Proposition 2.1] shows the existence of an invariant manifold contained within $\mathbb{X}^- \oplus \mathbb{X}^+ \oplus \mathbb{X}^{++}$ such that most solutions not exiting a neighborhood contained in $\mathbb{X}^- \oplus \mathbb{X}^+ \oplus \mathbb{X}^{++}$ near the strongly unstable subspace $\mathbb{X}^+ \oplus \mathbb{X}^{++}$ must lie beyond a parabola-shaped graph.

$\|\cdot\|_{**}$ – norm

Let $\epsilon > 0$. For $U = (u, v) \in L^2_{per}(\Omega) \times L^2_{per}(\Omega)$, U can be written as

$$U = \sum_{k=0}^{\infty} ((\alpha_{k,\epsilon}^+) E_{k,\epsilon}^+ + (\alpha_{k,\epsilon}^-) E_{k,\epsilon}^-) \cdot \psi_k.$$

- $E_{k,\epsilon}^{\pm} \cdot \psi_k$ are the eigenfunctions of the linearization of the mixed system subject to periodic boundary conditions
- ψ_k are the Fourier basis functions subject to periodic boundary conditions.

The norm $\|\cdot\|_{**}$ is defined as

$$\|U\|_{**}^2 = \sum_{k=0}^{\infty} (1 + \kappa_k)^{2\alpha} \left((\alpha_{k,\epsilon}^+)^2 + (\alpha_{k,\epsilon}^-)^2 \right).$$

Results

We show that the following are true:

- (H1), Lemma 4.3.1
- (H2), Lemma 4.3.2
- (H3), Lemma 4.3.3

Consider the spectrum associated with the linearization of the right hand side of the local system subject to homogeneous Neumann boundary conditions. For $0 < \beta \leq 1$, the spectrum associated with \mathcal{H}_ϵ is very similar. The proofs for (H2) and (H3) rely upon this similarity.

Eigenvalues of \mathcal{H}_ϵ for $0 \leq \beta \leq 1$ Lemma (Eigenvalues of \mathcal{H}_ϵ)

Suppose that previous assumptions are satisfied. The eigenvalues of \mathcal{H}_ϵ are

$$\lambda_k^\pm = \lambda^\pm(\epsilon\nu_k) = \frac{b_k(\epsilon\nu_k) \pm \sqrt{(b_k(\epsilon\nu_k))^2 - 4c_k(\epsilon\nu_k)}}{2}, \quad (7)$$

where

$$b_k = b(\epsilon\nu_k) = (f_u + g_v) - (d + 1)(\epsilon\nu_k)$$

$$c_k = c(\epsilon\nu_k) = (f_u g_v - g_u f_v) - (d f_u + g_v)(\epsilon\nu_k) + d(\epsilon\nu_k)^2,$$

and ν_k are the eigenvalues of $-\beta\Delta - (1 - \beta)(J_c - \hat{J}_0)$.

- See Lemma 4.2.1

Eigenvalues of $-\beta\Delta - (1 - \beta)(J_c - \hat{J}_0)$

For rectangular domains, the growth of eigenvalues of $-\Delta$ are given as

$$\kappa_k \sim k^{2/\dim \Omega}. \quad (8)$$

By a previous assumption, $J \in C^1(\bar{\Omega})$ and periodic. The eigenvalues of J_c are given as the Fourier coefficients of J and are denoted as \hat{J}_k . Thus, we have

$$\hat{J}_0 - \hat{J}_k \sim \hat{J}_0. \quad (9)$$

For $0 < \beta \leq 1$, $\nu_k \sim k^{2/\dim \Omega}$ and for $\beta = 0$, $\nu_k \sim \hat{J}_0$.

Spectrum of \mathcal{H}_ϵ (New)

Theorem (Spectrum of \mathcal{H}_ϵ)

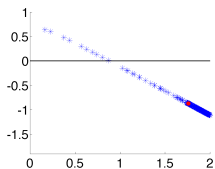
Suppose that the previous assumptions are satisfied. Let $\mathcal{H}_\epsilon : \mathbb{L}_{per}^2(\Omega) \rightarrow \mathbb{L}_{per}^2(\Omega)$ be defined as $\mathcal{H}_\epsilon = \epsilon D\mathcal{J} + B$, where D , \mathcal{J} and B are defined in Eqns. 4, 5 and 6, respectively. If $\beta = 0$, then the spectrum of \mathcal{H}_ϵ consists only of the eigenvalues \mathcal{H}_ϵ , the eigenvalues of the adjoint of \mathcal{H}_ϵ and the points $\lambda^\pm(\epsilon \hat{J}_0)$. If $0 < \beta \leq 1$, the spectrum contains only the eigenvalues of \mathcal{H}_ϵ .

- The space $\mathbb{L}_{per}^2(\Omega)$ is defined as $\mathbb{L}_{per}^2(\Omega) = L_{per}^2(\Omega) \times L_{per}^2(\Omega)$.
- See Theorem 4.2.1

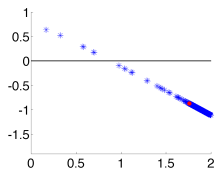
$\theta = 1$ case (New)

- As $\epsilon \rightarrow 0$, $\epsilon \nu_k \rightarrow \epsilon(1 - \beta)(\hat{J}_0 - \hat{J}_k)$.
- This behavior is responsible for removing the ϵ -dependent bound that forces the nonlinearity in the $\theta < 1$ case to be arbitrarily small as $\epsilon \rightarrow 0$.
- $R_\epsilon \sim \epsilon^{\alpha/\delta}$

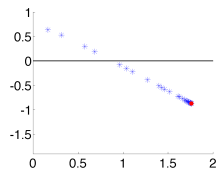
$\theta = 1$ case



(a) Large ϵ



(b) Medium ϵ



(c) Small ϵ

Figure: Eigenvalues of Linearized Right Hand Side for Periodic System

Numerical Experiment

- When the relative difference between the solution and its linearized counterpart reaches a tolerance of $\frac{1}{4}\epsilon^{1/4}$, the simulation is stopped and the distance of the solution to the homogeneous equilibrium is computed.
- Ω is assumed to be $\Omega = [0, 1] \times [0, 1]$.
- For each ϵ and β pair, 20 random initial conditions were used. The values of ϵ are 70 logarithmically spaced points between 10^{-5} and 10^{-3} .

Kernel

Consider the Gaussian kernel G defined as

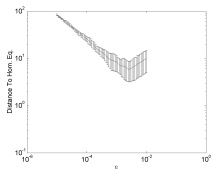
$$G(x, y) = \frac{C}{\epsilon} \exp\left(\frac{-x^2 - y^2}{\sigma^2}\right) \cdot \eta(x, y),$$

where $\eta(x, y)$ is a smooth cutoff function. The function η is 1 on $B_{1/3}(0, 0)$, but vanishes outside of $B_{1/2}(0, 0)$. The kernel $J(x, y)$ is given as the periodic extension of

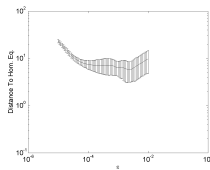
$$J(x, y) = \frac{C}{\epsilon} (G(x, y) + G(x+1, y) + G(x+1, y+1) + G(x, y+1)),$$

where $C = 200 \cdot \frac{s_r}{\pi}$. The constant s_r represents the right endpoint of the interval in which the eigenvalues of \mathcal{H}_ϵ are positive.

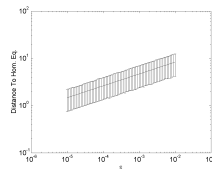
Results, $(C = 200 \cdot \frac{s_r}{\pi})$



(a) $\beta = 1.0$

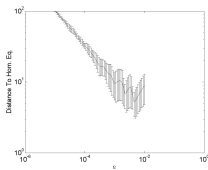


(b) $\beta = 0.875$

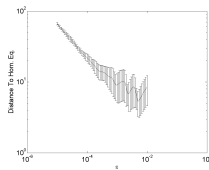


(c) $\beta = 0.0$

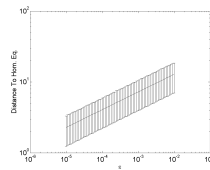
Results, $(C = 90 \cdot \frac{s_r}{\pi})$



(d) $\beta = 1.0$



(e) $\beta = 0.875$



(f) $\beta = 0.0$

Outline

- 1 Introduction
- 2 Early Pattern Selection
- 3 Summary**




Summary

- ($\theta < 1, 0 < \beta \leq 1$.) Results are presented showing that for reaction-diffusion systems with mixed nonlocal and local diffusion terms, the initial pattern selection is dominated by linear behavior. The methods can be applied to other related mixed local-nonlocal models.
- ($\theta = 1, 0 < \beta < 1$.) The initial pattern selection in the purely nonlocal case is dominated by nonlinear effects. Using the Gaussian kernel that was considered, the numerics indicate a large nonlinear influence for $\beta = 0$.




Acknowledgements

- Dr. Evelyn Sander, Department of Mathematics at GMU
- NSWCDD
- ONR

References I

-  V. Castets, J. Boissonade, and P. D. Kepper.
Experimental evidence of a sustained standing Turing-type nonequilibrium chemical pattern.
Phys. Rev. Lett., 64:2953–2956, 1990.
-  G. H. Gunarantne, Q. Ouyang, and H. L. Swinney.
Pattern formation in the presence of symmetries.
Phys. Rev. E, 50:2802–2820, 1994.
-  M. Hildebrand, H. Skødt, and K. Showalter.
Spatial symmetry breaking in the Belousov-Zhabotinsky reaction with light-induced remote communication.
Phys. Rev. Lett., 87(8):1–4, 2001.

References II

-  O. Jensen, V. Pannbacker, G. Dewel, and P. Borckmans.
Subcritical transitions to Turing structures.
Phys. Letters A, 179:91–96, 1993.
-  A. Kaminaga, V. Vanag, and I. Epstein.
"black spots" in a surfactant-rich Belousov-Zhabotinsky reaction dispersed in a water-in-oil microemulsion system.
J. of Chem. Phys., 122, 2005.
-  S. Maier-Paape and T. Wanner.
Spinodal decomposition of the Cahn-Hilliard equation in higher dimensions. part I: probability and wavelength estimate.
Comm. Math. Phys., 195(2):435–464, 1998.

References III



S. Maier-Paape and T. Wanner.

Spinodal decomposition for the Cahn-Hilliard equations in higher dimensions: nonlinear dynamics.

Arch. Rational Mech. Anal., 151(3):187–219, 2000.



J. D. Murray.

Mathematical Biology, Vol. I, An Introduction.

Springer–Verlag, New York, third edition, 1993.



Q. Ouyang and H. Swinney.

Transition from a uniform state to hexagonal and striped turing patterns.

Nature, 352:610–612, 1991.

References IV



V. K. Vanag and I. R. Epstein.

Pattern formation in a tunable reaction-diffusion medium: the BZ reaction in an aerosol OT microemulsion.

Phys. Rev. Lett., 87:1–4, 2001.



D. J. Wollkind and L. E. Stephenson.

Chemical Turing pattern formation analyses: comparison of theory with experiment.

SIAM J. Appl. Math., 61(2):387–431, 2000.